SPE

Society of Petroleum Engineers of AIME

SPE 8396

A FULLY IMPLICIT GENERAL PURPOSE FINITE-DIFFERENCE THERMAL MODEL FOR IN SITU COMBUSTION AND STEAM

by Janusz W. Grabowski, Paul K. Vinsome, Ran C. Lin, Alda Behie, and Barry Rubin, Members SPE-AIME, Computer Modelling Group

This paper was presented at the 54th Annual Fall Technical Conference and Exhibition of the Society of Petroleum Engineers of AIME, held in Las Vegas, Nevada, September 23-26, 1979. The material is subject to correction by the author. Permission to copy is restricted to an abstract of not more than 300 words. Write 6200 N. Central Expy., Dallas, Texas 75206.

ABSTRACT

This paper describes the development of a fully implicit general thermal model (ISCOM) for simulating in situ combustion or steam processes. The model includes four phases, a variable number of oil components, a variable number of chemical reactions, gravity and capillary pressure terms, and the possibility of modeling emulsions.

The finite-difference formulation of ISCOM operates in one, two or three dimensions and contains implicit and sequential implicit solution techniques as options. It is highly stable, averaging 30% saturation or molar fraction changes during each time step. The model includes the use of pseudo-phase equilibrium ratios which allows a single formulation, even though phases may disappear. The computer program was designed to emphasize clarity and to optimize storage. The matrix solution technique is a modified form of Gaussian elimination. The variables and fundamental equations have been aligned so that pivoting for numerical stability is not necessary. Other special features include Newtonian iteration with numerically calculated derivatives, embedding of the coke equation, two-point upstream and harmonic mobilities as options to reduce truncation error and the grid orientation effect, and an automatic time step selector. Results are presented showing the sensitivity to changes in number of grid blocks and time step size and showing the influence of harmonic weighting on the grid orientation effect.

INTRODUCTION

Thermal methods occupy a prominent position in the recovery of low API crudes. The processes taking place during thermal oil recovery are of a complex nature. Experience has shown that in order to model such processes, any numerical simulator must be extremely stable to produce practical results. The trend, therefore, has been towards increasing degrees of implicitness in the construction of such simulators. This demands, however, the utilization of large computer storage and run times, especially for multi-dimensional problems.

This paper describes the development of a fully implicit, finite-difference, general purpose thermal simulator (ISCOM) for modeling in situ combustion and steam processes. The storage and computation time problems have been resolved by the development of a special matrix band reducing option.

Another feature of thermal recovery simulations in heavy oils is the severity of the grid orientation effect. In ISCOM this effect is alleviated by an option which introduces harmonic mobility weighting.

The steam drive/soak options are subsets of the in situ combustion model, whereby unnecessary reactions and equations are removed. The steam versions are described here only briefly. Therefore this paper concentrates primarily on the in situ combustion option.

The formulation of the model, physical property package, and method of solution will be described, together with the results of some test calculations.

FORMULATION OF THE MODEL

Basic Assumptions

The mathematical model is based on the following assumptions:

1. The model can operate in one, two or three dimensions with variable grid spacing.
2. The number of components is variable, and components are distributed among four phases: water (w), oil (o), gas (g), and solid (c).
3. Water and oil components may be present in both oil and water phases, allowing for an approximate treatment of emulsions.
4. The number and type of chemical reactions is variable.

References and illustrations at end of paper.

5. Reservoir rock and fluids are compressible.

6. Capillary pressure and gravity terms are taken into account.

7. The reservoir is in thermodynamic equilibrium.

8. Interphase mass transfer takes place under equilibrium conditions.

9. Heat transport is through convection and conduction.

10. Heat loss to surroundings (normally cap and base rock) is included.

11. Diffusion is negligible.

12. Injection and production conditions for a given well are at constant rate, constant pressure or constant pressure limited by a maximum rate.

Simulator Equations

The set of the simulator equations is composed of continuity equations for each component, the energy conservation equation, algebraic constraints, and phase equilibrium relationships. The total number of components, N_c, consists of 1 water component, N_o oil components which are liquids at standard conditions (100 kPa, 15 °C), N_g gas components which are gaseous at standard conditions and 1 solid component i.e., coke. Therefore $N_c = 2 + N_o + N_g$. The sequence of components is as follows: water, oils (from heaviest to lightest), gases (oxygen last), and coke. An example of this sequence is presented in Table 1 for a minimal realistic set containing 6 components. Such a set is used for the calculations presented in this paper. The molar fractions X_{Li} in Table 1 show which non-zero equilibrium K-values have been used in the calculations.

The N_c-1 continuity equations for the fluid components are of the form:

$$- \nabla \sum_{L=1}^{3} X_{Li} C_L \vec{V}_L + \sum_{nr=1}^{NR} s_{nr,i} R_{nr} + Q_i = \frac{\partial}{\partial t} \phi^* \sum_{L=1}^{3} X_{Li} C_L S_L \quad i=1,\ldots,N_c-1 \quad \ldots (1)$$

where values 1, 2 and 3 of index L correspond to water, oil and gas phases. C_L is the molar density of phase L and $\vec{V}_L$ is the phase velocity:

$$\vec{V}_L = - k k_{rL} / \mu_L \nabla (P_L - G_L) \quad \ldots (2)$$

ϕ^* is the liquid phase porosity related to the total porosity ϕ through a factor accounting for the volume occupied by solid:

$$\phi^* = \phi (1 - C_c / C_c^\circ) \quad \ldots (3)$$

where C_c is the reservoir molar density of coke (number of moles of coke/total void volume of reservoir), and C_c° the molar density of pure coke.

The continuity equation for coke which is immobile is given by:

$$\sum_{nr=1}^{NR} s_{nr,N_c} R_{nr} = \frac{\partial}{\partial t} \phi C_c \quad \ldots (4)$$

The energy conservation equation contains convection, conduction, reaction, injection, production, and heat loss terms:

$$- \nabla \sum_{L} \bar{H}_L \vec{V}_L + \nabla \lambda_h \nabla T + \sum_{nr=1}^{NR} R_{nr} \bar{H}_{nr} + \sum_{i=1}^{N_c} Q_i \bar{HQ}_i - \bar{H}_{loss} = \frac{\partial}{\partial t} \left[\phi^* \sum_{L} C_L S_L \bar{U}_L + \phi C_c \bar{U}_c + (1 - \phi^*) C_R \bar{U}_R \right] \quad \ldots (5)$$

There are four constraint equations: one for saturations and three for molar fractions:

$$\sum_{L=1}^{3} S_L = 1 \quad \ldots (6)$$

$$\sum_{i=1}^{N_c} X_{Li} = 1 \quad L=1,\ldots,3 \quad \ldots (7)$$

The number of phase equilibrium equations depends on the number of components allowed to be present in more than one phase. The equations are of three types:

$$X_{gi} = X_{oi} K_{oi} \quad \ldots (8a)$$

$$X_{gi} = X_{wi} K_{wi} \quad \ldots (8b)$$

$$X_{oi} = X_{wi} K_{owi} \quad \ldots (8c)$$

Non-zero values of equilibrium constants K_{owi} allow for an approximate treatment of emulsion flow.

PHYSICAL PROPERTIES

Most of the physical properties of the model are expressed through standard correlations[1] and are presented in Table 2.

We will discuss here only the equilibrium K-values, which have the following special form for the water and oil components:

$$K_{w1} = 8.777\ 10^{-3} (T - 243)^{4.76} \frac{S_w}{P(S_w + \varepsilon_w)} \quad \ldots (9)$$

$$K_{o2} = \mathrm{Exp}\ AK_2 + BK_2/(T - CK_2) \frac{S_w}{P(S_o + \varepsilon_o)} \quad \ldots (10)$$

$$K_{oi} = \text{Exp}\ AK_i + BK_i/(T - CK_i) \qquad i=3,\ldots,N_o \qquad \ldots (11)$$

The water and heavy oil K-values have been multiplied by saturation dependent factors, introduced in reference 2, which avoid the need for variable substitution when one of the liquid phases disappears. A physical system with such pseudo K-values contains all three fluid phases at any pressure and temperature condition. However, the amount of a phase which in reality should not be present at any given set of conditions is very small and does not appreciably influence the behaviour of the system.

The emulsion simulating K-values K_{owi} in relation (8c) are not specified at present because of lack of data and are set to zero.

Chemical Reactions

Each chemical reaction between N_c components a_i is represented by the equation:

$$\sum_i s_{nr,i}\, a_i = \sum_i s^*_{nr,i}\, a_i \qquad nr=1,\ldots,NR \qquad \ldots (12)$$

Chemical reactions between the same components in different phases are considered as separate reactions.

The rate for reaction nr is expressed as:

$$R_{nr} = r_{nr}\, \text{Exp}(-E_{nr}\, RT) \prod_m (D_{Lm})^{e_m} \qquad \ldots (13)$$

where the index m encompasses all reacting components with non-zero stoichiometric coefficients on the left-hand side of equation (12).

The density factors D_{Lm} are equal to:

$$D_{Lm} = \phi^*\, X_{Lm}\, C_L\, S_L \qquad \ldots (14)$$

except for the oxygen density factor $D_{g,\text{oxygen}}$ which is normally expressed through the partial pressure of oxygen:

$$D_{g,\text{oxygen}} = X_{g,\text{oxygen}}\, P_g \qquad \ldots (15)$$

The ISCOM program allows a choice between expression (14) or (15) for $D_{g,\text{oxygen}}$.

Well Model

Each of the injection or production wells can operate in one of the following modes:

a) shut in
b) constant rate
c) constant pressure
d) constant pressure limited by maximum rate.

Production rates for each well are calculated from mobilities in production blocks. In case d) the rate is calculated first as a pressure constrained value then compared with the maximum allowable rate and the smaller of the two is used in calculations.

Heat Loss

Heat loss to the environment surrounding the reservoir is calculated from the numerical solution of the heat conduction equation by a semi-analytical method similar to that developed in reference 3.

The options in ISCOM allow for separate calculations of heat loss to surrounding environment from each side of the reservoir, and backflow of heat is allowed.

Upstream and Harmonic Options

With the standard single-point upstream approximation, the mobility is evaluated fully implicitly. However, if two-point upstream is required, this cannot be done without increasing the bandwidth of the Jacobian matrices. Therefore for two-point upstream a similar but rather simpler formulation than given in reference 4 is used.

The mobility between grid blocks j and j+1 is given by:

$$\lambda^{k+1}_{j+\frac{1}{2}} = \lambda^{k+1}_j + \frac{\Delta x}{2}\,\frac{\lambda^{\nu}_j - \lambda^{\nu}_{j-1}}{\Delta x} \qquad \ldots (16)$$

where the iteration level ν may be taken at the old time level n, or the latest iterate k. The normal maximum and minimum overshoot constraints[5] are implemented on the slope term $(\lambda^{\nu}_j - \lambda^{\nu}_{j-1})/\Delta x$. It has been found through experience that n level is normally sufficient, and does not appreciably affect the stability. If k level is chosen it should be limited to the first two or three Newtonian iterations otherwise the overshoot constraints can cause slow convergence.

Both single-point and two-point upstream give severe grid orientation effects during in situ combustion simulations. They are even worse than in previously published results for steam drive[6]. The harmonic total mobility approximation developed in reference 7 specifically to reduce grid orientation effects, is also available as an option in the present simulator. The approximation in its simplest form, which is based on the assumption of a short transition zone between grid nodes, involves the modification of the individual phase mobilities λ_L by the factor $2 \times \lambda_{Tu}/(\lambda_{Tu} + \lambda_{Td})$, where λ_{Tu} and λ_{Td} represent upstream and downstream total mobilities. In the results section of the paper, it is shown that the use of harmonic mobilities greatly alleviates the grid orientation effect during areal in situ combustion simulations.

SOLUTION METHOD

Choice of Independent Variables

Based on the same rationale as given in reference 1, the choice of independent variables is taken as: P, S_w, S_o, T, X_{g,N_g}, $X_{g,i}(i=N_o+2,\ldots,N_g-1)$, $X_{o,i}(i=2,\ldots,N_o-1)$.

The gas saturation is not an independent variable, but is obtained from the saturation constraint (6).

The first N_o gas molar fractions are calculated from relations (8a) and (8b). From the rest of the $N_g - N_o$ variables, $N_g - N_o - 1$ gas molar fractions are independent variables and one - the inert gas component or nitrogen - is calculated from the gas molar fraction constraint (7). The ordering of independent gas molar fraction variables is: first oxygen (or component number N_g) followed by any combustion gases (CO, CO_2) or non-condensable hydrocarbons. In the six-component model there is only one independent gas molar fraction: $X_{g,oxygen}$.

The oil molar fractions are ordered from heaviest to lightest, the lightest molar fraction being evaluated from the oil molar fraction constraint (7).

Not only is the choice of independent variables important, but also the exact ordering as given above is essential for the success of the bandwidth reducing option described in the section on discretization and iteration scheme.

Embedding of the Coke Equation

A notable feature of the choice of independent variables was the omission of the reservoir molar coke density C_c. The coke calculation has been removed from the set of independent variables, and embedded into the physical property package as follows.

The coke equation (4) is of the form:

$$\frac{\partial}{\partial t}(\phi\, C_c) = \sum_{rc} s_{rc} R_{rc} - \sum_{rb} s_{rb} R_{rb} \quad \ldots (17)$$

where R_{rc} are the coke producing cracking reactions and R_{rb} the coke burning reactions. The two types of reactions have the following functional dependencies on the reservoir coke density C_c:

$$\sum_{rc} s_{rc} R_{rc} = A_1 \left(1 - \frac{C_c}{C_c^\circ}\right)$$

$$\sum_{rb} s_{rb} R_{rb} = A_2 (C_c)^{e_m}$$

where A_1 and A_2 are functions of other independent variables, but not of the coke molar density. The exponent e_m is frequently taken as unity, but can also be slightly different than unity.

Equation (17) can be written to first order in time as:

$$\frac{\phi^{n+1} C_c^{n+1} - \phi^n C_c^n}{\Delta t} = A_1 (1 - C_c^{n+1} C_c^\circ)$$

$$- A_2 C_c^{n+1} (C_c^k)^{e_m - 1} \quad \ldots (18)$$

where the superscript k represents the latest level of the Newtonian iteration. Rearrangement gives an algebraic expression for the coke density:

$$C_c^{n+1} = \frac{\phi^n C_c^n + \Delta t\, A_1}{\phi^{n+1} + \frac{\Delta t\, A_1}{C_c^\circ} + \Delta t\, A_2 (C_c^k)^{e_m - 1}} \quad \ldots (19)$$

Thus the calculation of the reservoir molar coke density has been reduced to the evaluation of a simple algebraic function, and can be treated in the same manner as the physical properties.

Discretization and Iteration Scheme

The conservation equations are discretized into finite-difference form using first order backward differences in time, and central differences in space with upstream densities, mobilities, and enthalpies in the flow terms.

The discretized equations at each grid node are written in functional form:

$$F_j(f_{ki}) = 0 \qquad j=1,\ldots,N_c \qquad k=1,\ldots,N_c$$

$$i=1,\ldots,N \quad \ldots (20)$$

where f_{ki} represents the independent variables.

The equations are solved fully implicitly by Newtonian iteration. This requires computation of the Jacobian matrix of derivatives, of which one block line is given by $\partial F_j / \partial f_{ki}$ where k runs over all the independent variables and i the grid nodes. The derivatives are evaluated numerically. The resulting Jacobian matrix is block banded, having 3, 5 or 7 block bands depending on the number of dimensions. Solution is for the change of the independent variables over an iteration. The Jacobian matrix is inverted using a backward Gaussian elimination and forward substitution. Testing for zero downstream entries is performed during the elimination to reduce the computational work. Normally about 4 Newtonian iterations are required per time step. The inclusion of two-point upstream weighing without increasing the bandwidth of the Jacobian matrices is discussed in section "Upstream and Harmonic Options". When wells are completed through more than one grid block a similar successive substitution procedure to the two-point upstream is used to avoid increasing the matrix bandwidth. Under these circumstances, the simulator should be termed highly implicit rather than fully implicit.

When the number of grid points becomes large most of the computation time is spent in solving the sets of simultaneous equations. A bandwidth reducing scheme (or sequential implicit scheme at the matrix level) was developed in reference 8 and tested in one dimension. This has since been extended to, and tested, in two and three dimensions. The scheme works as follows: Figure 1 represents one block line of the Jacobian matrix for a two-dimensional problem. The elements marked '0' are assumed to be negligible and are not computed. The elements marked 'G' are eliminated by Gaussian elimination on the block line. The elements denoted by 'D' then form a completely decoupled submatrix which can be solved separately with a much reduced bandwidth. The elements marked 'X' are then used in a procedure akin to forward substitution

to determine the remaining independent variables. Typically (P, S_w, S_o) or (P, S_w, S_o, T) are included in the submatrix.

The method saves on both storage and computing time. Some typical examples of computing time compared with the fully implicit solution are given in Table 3. The numbers refer to the overall run time of the simulator, including for example, all extra iterations required per time step when using the bandwidth reducing option.

Automatic Time Step Selection

During in situ combustion simulations the changes between time steps are so dramatic that some form of automatic time step selection is essential. It is impossible to run the program with a constant time step, unless the chosen time step is extremely small.

In this simulator the time step is estimated by comparing the maximum changes of independent variables during the previous time step δ_i, with input norms η_i and:

$$\Delta t^{n+1} = \Delta t^n \min_i \frac{(1+w)\eta_i}{\delta_i + w\,\eta_i} \qquad \ldots (21)$$

where index i runs over pressure, temperature, all saturations, and all molar fractions; w is a damping factor whose optimum value has been found through experience to be around unity. If a linear extrapolation is used (i.e., w = o) the time step is invariably underestimated if $\delta > \eta$, and overestimated is $\delta < \eta$.

The formula given cannot increase the time step ratio $\Delta t^{n+1}/\Delta t^n$ by more than a factor 2. If the predicted ratio is less than 0.5 the time step is automatically repeated with half of the time step value. Therefore changes of up to three times the norm are allowed. Typical norms are 20% for saturations and molar fractions, 40 °C for temperature, and 500 kPa for pressure. This means that during a typical run variations of up to 60% can be observed, especially in changes of molar fractions. The simulator is robust enough to tolerate changes of up to 90% over a time step.

Generally it requires 4 to 5 Newtonian iterations to achieve convergence on saturations and molar fractions to better than 0.001 in every grid block. The number of iterations needed is not strongly dependent on the time step size. The time step ratio $\Delta t^{n+1}/\Delta t^n$ is computed during every Newtonian iteration except the first, to decide if the time step should be repeated. The reason for omitting the first iteration is that massive changes can occur (molar fractions of magnitude several hundred), while the subsequent iterations give convergence with changes around the norms. As it is clear that during the Newtonian iterations values of the dependent variables outside the physical domains can be computed, the property package must be defined over a wide range of these variables. As a general rule, when variables deviate outside the physical domain they are not set equal to the physical limits as this appears to spoil the convergence characteristics of the Newtonian iteration.

Steam Drive

Steam drive can be performed in several ways using ISCOM. One option removes the oxygen molar fraction and corresponding continuity equation from the equation set. The inert gas equation is still in the system and can be used to simulate a non-condensable hydrocarbon gas. However we observed some problems with this formulation during radial huff and puff simulations. The nitrogen molar fraction was reduced almost to zero by the large steam throughput in the production grid blocks. Then when the steam zone collapsed the Newtonian iteration converged to answers in the unphysical region (the nitrogen molar fraction went negative, and the steam molar fraction was greater than 1). No matter how small a time step was used the same phenomenon occurred. The problem was finally resolved by the somewhat artificial device of switching on the low temperature cracking reaction so that small amounts of inert gas were generated in the system.

An alternative approach which has proved very successful is to use an equation substitution for the pressure. The nitrogen equation is removed from the system altogether. If gas is present the pressure variable is aligned on the molar fraction constraint:

$$\sum_{i=1}^{N_g} X_{gi} = 1 \qquad \ldots (22)$$

If no gas is present it is aligned on the saturation constraint:

$$S_o + S_w = 1 \qquad \ldots (23)$$

The conditions for switching from one equation to the other are as follows. If no gas is present and the iteration converges with $\sum_{i=1}^{N_g} X_{gi} > 1$ switch to the molar fraction constraint. If gas is present and the iteration converges with $S_g < 0$ switch to the saturation constraint. No difficulties have been observed with the switching process. The advantages of this scheme are that the independent variables are always the same, and the matrix structure remains invariant. Both steam formulations may be used with a variable number of oil components, including also the case of only one oil component in the system.

RESULTS

The performance of ISCOM has been studied on one, two and three dimensional simulations. Tests have been performed to find out the accuracy and sensitivity of the model with changes in the number of grid blocks, time step size and discretization directions (grid orientation effects). In all tests the heat loss was set to zero to facilitate comparison of the finite-difference scheme with other in situ combustion simulators. Also the harmonic mobility weighting was not included except for tests concerning the grid orientation effect.

The results of the grid sensitivity tests are presented in Figures 2 to 9. The data are given in Table 2. Figures 2, 3, 4 and 5 show temperature, gas saturation and oil production curves for one-

dimensional simulations with the reservoir represented by 10, 20 or 30 grid blocks with 30% norms for saturations and molar fractions. The maximum difference between the curves is of order of 10% with a deviation of order of one block in temperature distribution. A similar situation can be seen in the two-dimensional production curves in Figures 6 and 7 for a confined 1/4 five-spot pattern. Light oil production is more sensitive to grid size than heavy oil production. The results of Figures 8 and 9 show that grid sensitivity is not strongly affected by the inclusion of two-point upstream mobility weighting.

The time step sensitivity of ISCOM has been investigated in runs with different values of norms η_i determining time step selection in relation (21). The one-dimensional results are shown in Figures 10, 11, 12 and 13, and the two-dimensional results in Figures 14 and 15. Again the production curves coincide within 10% but front position varies by up to two grid blocks. The curves in Figures 16 and 17 show the results of using the two-point upstream option and also of using a very small saturation and molar fraction norm value of 5%. Calculations obtained with this small value of norm deviate quite strongly from the close group of results obtained with norms of 15, 20 and 30%. A run with norms set at 2.5% gave almost the same result as the 5% run. The exact reason for this sensitivity to time step size at values of norms in the range 2.5 - 15% is not yet known. Sensitivity to the reaction terms was tested by evaluating these terms with central differences in temperature, but the spread was only reduced to about 2/3 that shown in Figures 16 and 17. Investigation of this phenomenon is still continuing.

The effect of reduction of grid orientation in two-dimensional areal calculations is shown in Figures 18, 19, 20 and 21. Figures 18 and 20 show water saturation profiles and diagonal gas saturation cross-sections obtained with pure single-point upstream weighting. The severe grid orientation effect produces unphysical fingers; holes in saturation distributions are seen. In some runs even two holes like the one in Figure 18 have been observed. This grid orientation effect is much stronger than in steamflood simulations.

A drastic improvement is obtained when using the previously described option of one-point upstream with harmonic mobility weighting. The results are shown in Figures 19 and 21 for the same simulations as presented in Figures 18 and 20. The region of 40% water saturation in Figure 19 shows the condensation bank. The shape and advance of the front in Figure 21 looks much more realistic.

The utilization of harmonic mobility weighting does not remove all grid orientation effects as it is seen from Figure 22 and Figure 23 where the runs with diagonal and parallel grids are compared. However the discrepancies are within reasonable limits.

When the saturation and molar fraction norms are greater than about 50% ISCOM becomes unstable. The Newtonian scheme in such cases is starting too far from the final answer to be able to find a solution.

CONCLUSIONS

1. It has been shown that ISCOM is an effective and robust computer model for simulation of in situ combustion or steamflooding.
2. ISCOM has flexible physical and chemical property packages.
3. The fully implicit formulation of the solution method guarantees simplicity of programming, robustness in time step size with up to 50% norms in saturations and molar fractions. It demands however relatively large computing time and storage for higher dimensional runs.
4. The above time and storage limitations are greatly relaxed by the use of a band reducing option which can tolerate saturation and molar fraction norms of up to 30%.
5. The two-point upstream weighting scheme is easily implemented into ISCOM and produces little sensitivity in one-dimensional runs. Its effect on two and three-dimensional simulations will be investigated in the future.
6. The implementation of harmonic mobility weighting in ISCOM resulted in a great reduction of grid orientation effects.
7. The alignment of independent variables and equations is such that pivoting of the solution matrix is not necessary.

ACKNOWLEDGEMENTS

This research was supported by the Alberta/Canada Energy Resources Research Fund administered by the Department of Energy and Natural Resources of the Province of Alberta. It was brought to the attention of the authors that the theory for the bandwidth reducing option was developed independently by J.H. Abou-Kassem and is to be presented in a Ph.D. thesis[9]. The authors are thankful to Dr. K. Aziz for helpful discussions.

NOMENCLATURE

- a = component participating in chemical reaction
- A = coefficient in formula for critical saturation (°K)
- AK = coefficient in formula for K-values
- AV = coefficient in formula for oil viscosity (kPa day)
- BK = coefficient in formula for K-value (°K)
- BV = coefficient in formula for oil viscosity (°K)
- C = molar density (mol/m^3)
- CK = coefficient in formula for K-value (°K)
- C_p = specific heat (J/mol °K)
- e = power in formula for reaction rate
- E = activation energy (KJ/mol)
- f_{ki} = independent variable i in block k
- F_j = functional for discretized form of equation j

G = gravity term in continuity equation kPa

$\overline{H}$ = specific enthalpy (J/mol)

$\overline{HQ}$ = specific enthalpy of injection or production (J/mol)

$\overline{H}_v$ = specific enthalpy of vaporization (J/mol)

HO = heavy oil

IG = inert gas

k = absolute permeability (m^2)

k_r = relative permeability

K = equilibrium K-value

LO = light oil

M = molar mass (kg/mol)

N = number of components

P = pressure

Q = injection or production rate (mol/m^3 day)

R = gas constant = 8.314 10^{-3} kJ/mol °K

R_{nr} = reaction rate (mol/m^3 day)

r = frequency coefficient in reaction rate (kPa day)$^{-1}$

S = saturation

s = stoichiometric coefficient of reactant

s* = stoichiometric coefficient of product

S_c = critical saturation

t = time

T = temperature (°K)

T_c = temperature in °C

T_{cr} = critical temperature (°K)

T_s = coefficient in formula for critical saturation (°K)

$\overline{U}$ = specific internal energy (J/mol)

$\vec{V}$ = phase velocity (m/day)

X = molar fraction

Z = gas compressibility factor

α = compressibility factor (kPa)$^{-1}$

β = thermal expansion factor (°K)$^{-1}$

δ = maximum changes of independent variables (units of the variables)

ϵ = coefficient in formula for K-value

η = input norms of independent variables (units of the variables)

λ = mobility (m^2/kPa day)

λ_h = heat conductivity (J/m day °K)

μ = viscosity (kPa day)

σ = coefficient in formula for critical saturation

ϕ = total porosity

ϕ^* = liquid phases porosity

Subscripts and Indices

c = coke

g = gas

i = component

j = block number

k = iteration time level

L = phase number (1-water, 2-oil, 3-gas)

m = index for non-zero stoichiometric coefficient of chemical reactant

n = time level

nr = number of chemical reactant

NR = total number of chemical reaction

o = oil

ov = over or under burden

R = rock

rb = number of burning reactions

rc = number of cracking reactions

w = water

REFERENCES

1. Reid, R.C., Prausnitz, J.M. and Sherwood, T.K.: "The Properties of Gases and Liquids," McGraw-Hill Book Co., N.Y., 1977.

2. Crookston, R.B., Culham, W.E. and Chen, W.H.: "A Numerical Simulation Model for Thermal Recovery Processes," Soc. Pet. Eng. J. (Feb. 1979), 37-58.

3. Chase, C.A. and O'Dell, P.M.: "Application of Variational Principles to Cap and Base Rock Heat Losses," Trans., AIME, Vol. 255 (1973), 200-210.

4. Wheatley, M.J.: "A Version of Two-Point Upstream Weighting for Use in Implicit Numerical Reservoir Simulators," SPE 7677, Proc. Fifth SPE Symp. on Res. Sim., Denver, 1979.

5. Holloway, C.C., Thomas, L.K. and Pierson, R.G.: "Reduction of Grid Orientation Effects in Reservoir Simulation," Paper SPE 5522 presented at 50th Annual Fall Meeting, Dallas, 1975.

6. Coats, K.H., George, W.D., Chieh Chu and Marcum, B.E.: "Three Dimensional Simulation of Steamflooding," Paper SPE 4500 presented at 48th Annual Fall Meeting, Las Vegas, 1973, Trans., AIME, (1973), Vol. 257, II 573-592.

7. Vinsome, P.K.W. and Au, A.D.K.: "One Approach to the Grid Orientation Problem in Reservoir Simulation," Paper SPE 8247 presented at the SPE-AIME 54th Annual Fall Technical Conference and Exhibition, Las Vegas, Sept. 1979.

8. Rubin, B. and Vinsome, P.K.W.: "The Simulation of the In Situ Combustion Process in One Dimension Using a Highly Implicit Finite-Difference Scheme," Paper no. 79-30-14 presented at 30th Annual Technical Meeting of Pet. Soc. of CIM, Banff, 1979.

9. Abou-Kassem, J.H.: "Investigation of Grid Orientation in a Two-Dimensional Compositional Three-Phase Steam Model," A Ph.D. Thesis (to be published), Dept. of Chem. Eng., University of Calgary, 1979.

TABLE 1
Sequence and Phase Distribution
for Case of 6 Components

Component	Gas Phase	Oil Phase	Water Phase	Solid Phase
1. Water	$X_{g,1}$		$X_{w,1}$	
2. Heavy Oil	$X_{g,2}$	$X_{o,2}$		
3. Light Oil	$X_{g,3}$	$X_{o,3}$		
4. Inert Gas	$X_{g,4}$			
5. Oxygen	$X_{g,5}$			
6. Coke				C_c

TABLE 2

Correlations for Physical Properties
and Data for 6 Component Case

Reservoir Dimensions

Length 72.73 m

Width 72.73 m

Depth 6.40 m

Porosity

$\phi = \phi_R [1 + \alpha(P - P_R)]$

$\phi_R = .38$

$\alpha = 0.\ kPa^{-1}$

$P_R = 100$ kPa

Equilibrium K-values

$AK_2 = 14.06$

$BK_2 = -3744$ °K

$CK_2 = 92.85$ °K

$AK_3 = 13.71$

$BK_3 = -1872$ °K

$CK_3 = 25.16$ °K

$\epsilon_w = \epsilon_o = 10^{-3}$

Relative Permeability

$k_{rL} = k_{rL}^* [(S_L - S_{cL})/(1 - S_{cL}')]^{e_L}$ $S_L \geq S_{cL}$

$k_{rL} = 0$ $S_L < S_{cL}$

$S_{cL} = S_{cL}^*/(1 + AS_L) + S_{cL}^1$

$AS_L = \text{Exp}\ [(\alpha_L T + T_{sL})/A_L]$

	k_{rL}^*	e_L	S_{cL}^*	S_{cL}^1	α_L
water	.25	3	0	0.2	1
oil	1.00	3	0	0.3	-1
gas	.70	2	0	0.5	1

Absolute Permeability

$k_x = k_y = k_z = 4.10^{-12}\ m^2$

Molar Density

water: $C_w = C_{wR} [1 + \alpha_w(P - P_R) - \beta_w(T - T_R)]$

$C_{wR} = 5.55\ 10^4$ mol/m³

$\alpha_w = 4.5\ 10^{-6}\ kPa^{-1}$

$\beta_w = 2.1\ 10^{-4}\ (°K)^{-1}$

$T_R = 298$ °K

oil: $C_o = C_{oR} [1 + \alpha_o(P - P_R) - \beta_o(T - T_R)]$

$C_{oR} = (\Sigma\ X_{oi}/C_{oR}^i)^{-1}$

$C_{oR}^2 = 4.16\ 10^3$ mol/m³

$C_{oR}^3 = 8.37\ 10^3$ mol/m³

$\alpha_o = 8.0\ 10^{-6}\ kPa^{-1}$

$\beta_o = 2.0\ 10^{-4}\ (°K)^{-1}$

gas: $C_g = P/RTZ$

$Z = 1$

Molar Mass

$M_L = \Sigma\ X_{Li} M_i$

$M_1 = 18.02\ 10^{-3}$ kg/mol

$M_2 = 170.0\ 10^{-3}$ kg/mol

$M_3 = 44.0\ 10^{-3}$ kg/mol

$M_4 = 40.3\ 10^{-3}$ kg/mol

$M_5 = 32.0\ 10^{-3}$ kg/mol

$M_6 = 12.0\ 10^{-3}$ kg/mol

Viscosity

water: $\mu_w = 10^{-9}/(12.1 + 2.88\ T_c + 7.78 \times 10^{-4}\ T_c^2)$ kPa day

oil: $\mu_o = \Pi(\mu_{oi})^{X_{oi}}$

$\mu_{oi} = AV_i\ \text{Exp}(BV_i/T)$

$AV_2 = 4.19\ 10^{-15}$ kPa day

$BV_2 = 4714$ °K

$AV_3 = 2.41\ 10^{-13}$ kPa day

$BV_3 = 533.1$ °K

gas: $\mu_g = 10^{-13}(1.574 + 44 \times 10^{-2} T_c)$ kPa day

Capillary Pressure

$P_{cw} = AC_{w1} + AC_{w2}\ S_w$

$P_{cg} = AC_{g1} + AC_{g2}\ S_g$

$AC_{w1} = AC_{w2} = AC_{g1} = AC_{g2} = 0$

Reservoir Conductivity

$\lambda_h = (1 - \phi^*)\ \lambda_{hR} + \phi^* \sum_L S_L\ \lambda_{hL}$

$\lambda_{hR} = 2.179\ 10^5$ J/day m °K

$\lambda_{hL} = 0$

Enthalpy and Internal Energy

$\overline{H}_L = \Sigma\ X_{Li}\ \overline{H}_{gi} - \overline{H}_{vL}$

$\overline{H}_{gi} = C_{pi}(T - T_R)$

$C_{p1} = 33.5$ J/mol °K

$C_{p2} = 242.0$ J/mol °K

$C_{p3} = 482.0$ J/mol °K

$C_{p4} = 46.0$ J/mol °K

$C_{p5} = 32.2$ J/mol °K

$C_{p6} = 17.0$ J/mol °K

$\overline{H}_{vw} = 4.814\ 10^3\ (T_{crw} - T)^{.38}$ J/mol $T \leq T_{crw}$

$\overline{H}_{vw} = 0$ $T > T_{crw}$

$\overline{H}_{vo} = 5.580\ 10^3\ (T_{cro} - T)^{.38}$ J/mol $T \leq T_{cro}$

$\overline{H}_{vo} = 0$ $T > T_{cro}$

$\overline{H}_{vg} = 0$

$\overline{U}_L = \overline{H}_L - 10^{-3}\ P_L/C_L$

$C_R \overline{U}_R = 2.35\ 10^6\ (T - T_R)$ J/m³

Heat Loss Data

$T_{ov} = 367$ °K

$\lambda_{ov} = 2.179\ 10^5$ J/day m °K

$C_{pov}\overline{U}_{ov} = 2.35\ 10^6$ J/m³

Injection - Production Data

Pure oxygen injected at constant rate 61 m³/day in block number 1.
Production at constant pressure 410 kPa in last block.

Chemical Reactions

There are 4 chemical reactions.

1. Light oil (LO) oxidation:

   $LO + 5O_2 = 4H_2O + 3IG$

2. Heavy oil (HO) oxidation:

   $HO + 18O_2 = 13H_2O + 12IG$

3. Cracking reaction:

   $HO = 2LO + 1.33IG + 4.67C$

4. Coke burning reaction:

   $C + 1.25O_2 = .5H_2O + IG$

nr	r_{HR} (kPa day)$^{-1}$	e_1	e_2	E_r kJ/mol	$\overline{H}_R$ J/mol
1	$1.45\ 10^5$	1	1	77.46	$2.21\ 10^6$
2	$1.45\ 10^5$	1	1	77.46	$8.12\ 10^6$
3	$3.00\ 10^5$*	1		66.99	$4.65\ 10^4$
4	$1.45\ 10^5$	1	1	54.43	$5.23\ 10^5$

*units day^{-1}

Initial Data

P	= 455 kPa	X_{o2}	= .9999
T	= 367 °K	X_{o3}	= .0001
S_w	= .30	X_{g5}	= 10^{-5}
S_o	= .69	C_c	= 0.
S_g	= .01		

TABLE 3

Time and Storage Saving for
Band Reducing Option (PSS) (TYX)

Model	Time Saving %	Storage Saving %
7x7 areal combustion	32	35
10x10 areal combustion		41
11x7x2 3-phase black oil	61	64

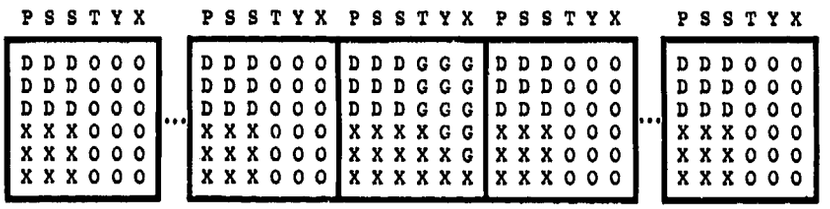

Fig. 1 - One block line of Jacobian matrix.

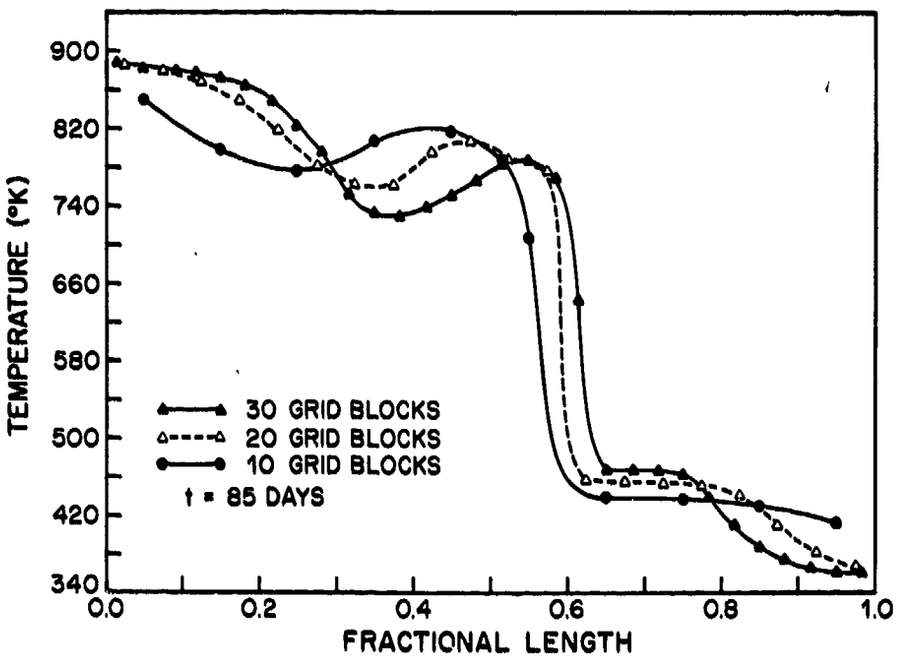

Fig. 2 - Grid size sensitivity. One-dimensional reservoir.

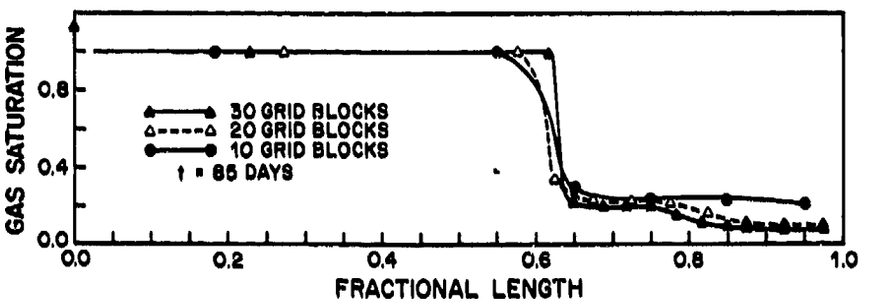

Fig. 3 - Grid size sensitivity. One-dimensional reservoir.

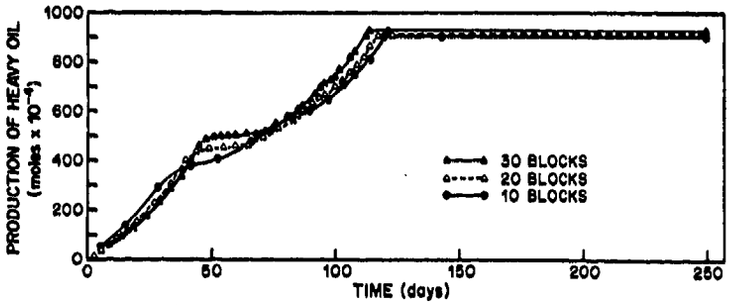

Fig. 4 - Grid-size sensitivity. One-dimensional reservoir.

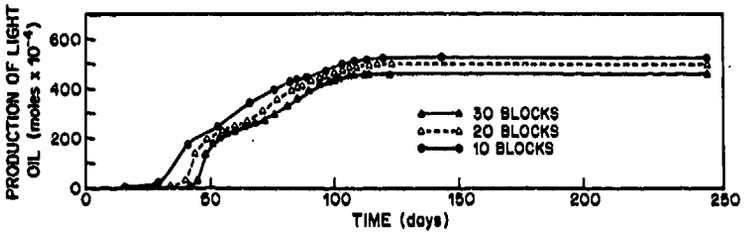

Fig. 5 - Grid size sensitivity. One-dimensional reservoir.

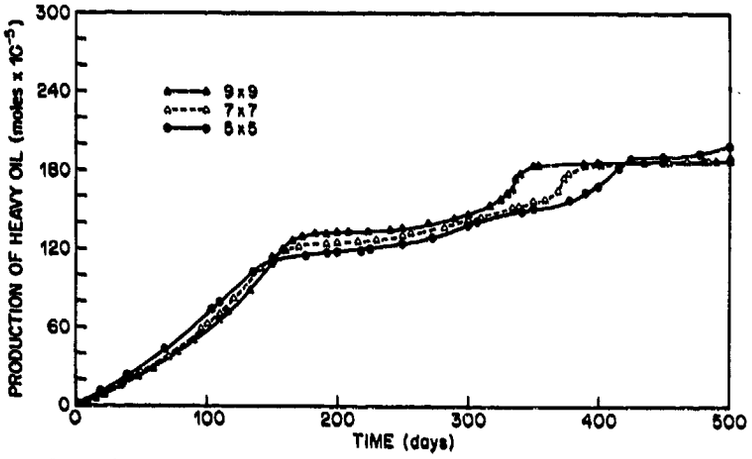

Fig. 6 - Grid-size sensitivity. Two-dimensional reservoir.

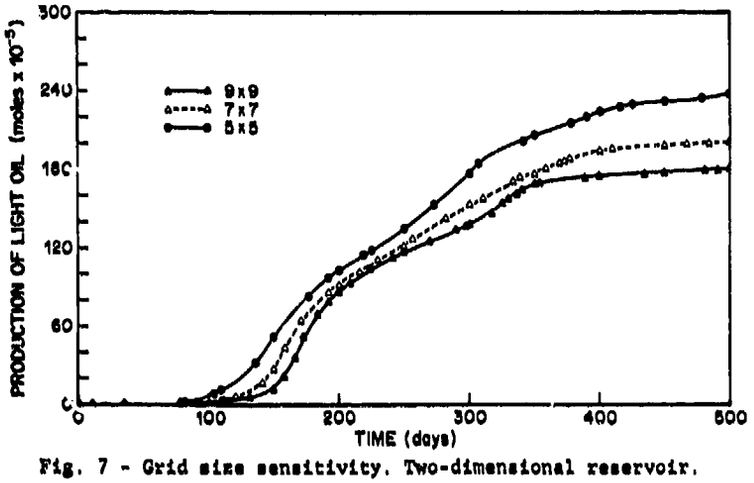

Fig. 7 - Grid size sensitivity. Two-dimensional reservoir.

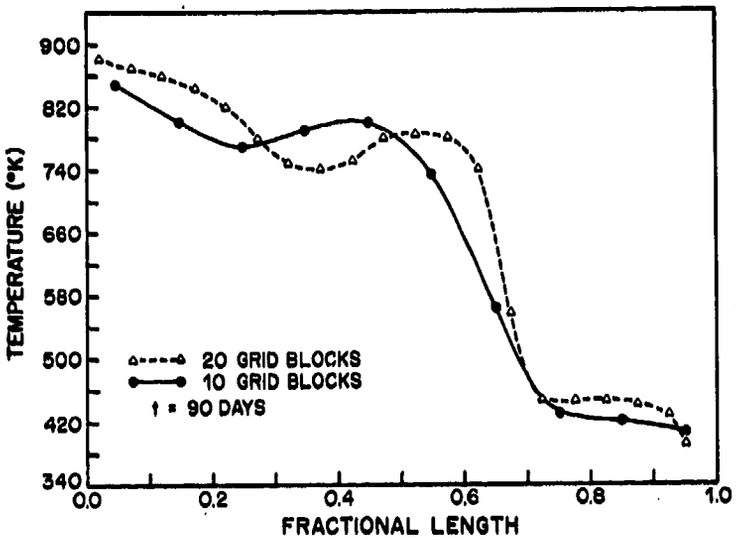

Fig. 8 - Effect of two-point mobility weighting on grid size sensitivity. One-dimensional reservoir.

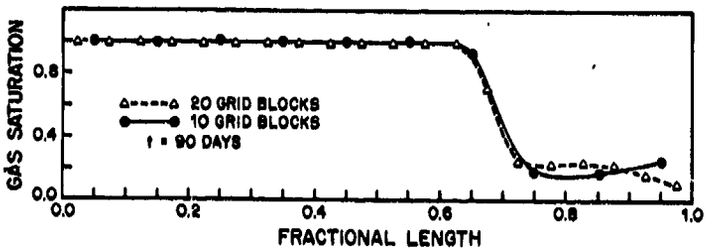

Fig. 9 - Effect of two-point mobility weighting on grid size sensitivity. One-dimensional reservoir.

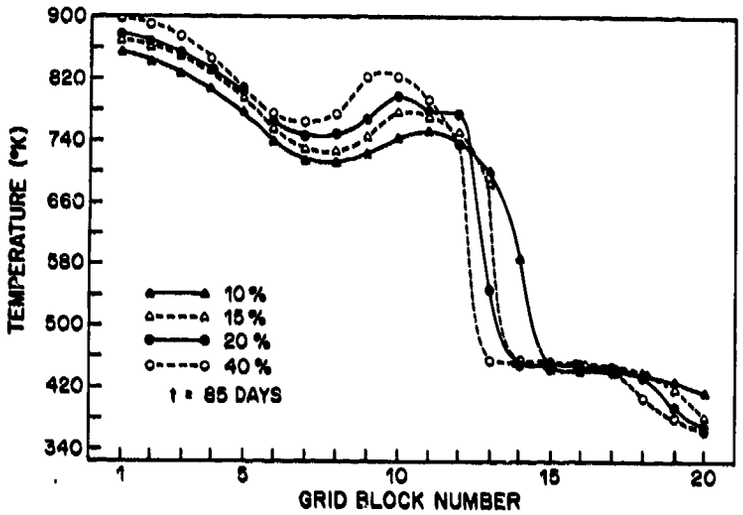

Fig. 10 - Time step sensitivity. One-dimensional reservoir.

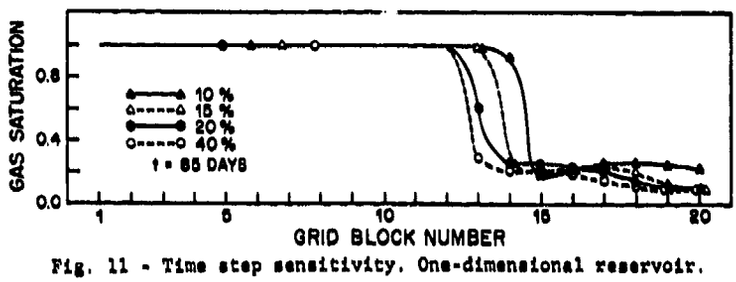

Fig. 11 - Time step sensitivity. One-dimensional reservoir.

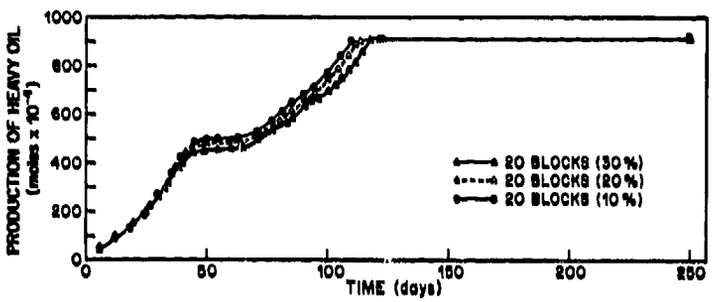

Fig. 12 - Time step sensitivity. One-dimensional reservoir.

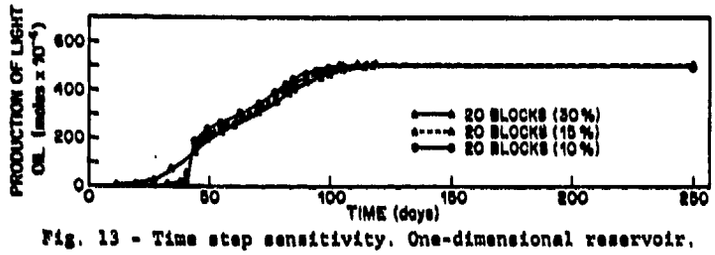

Fig. 13 - Time step sensitivity. One-dimensional reservoir.

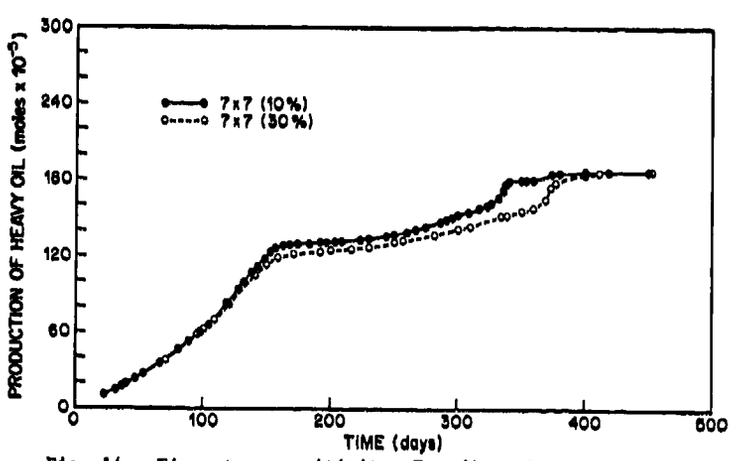

Fig. 14 - Time step sensitivity. Two-dimensional reservoir.

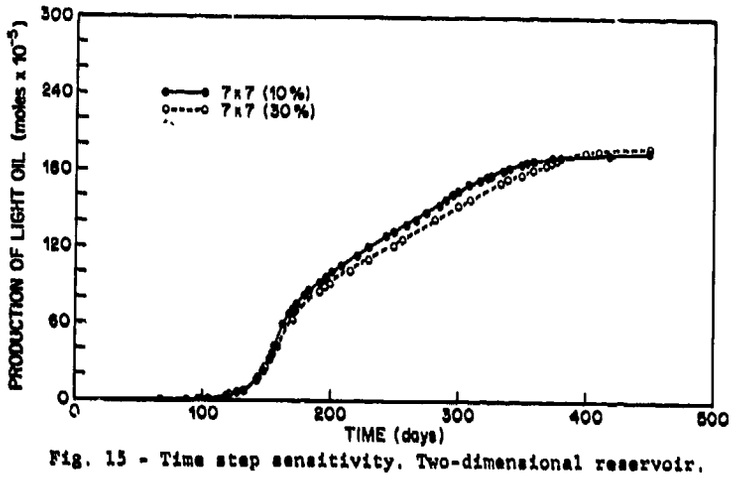

Fig. 15 - Time step sensitivity. Two-dimensional reservoir.

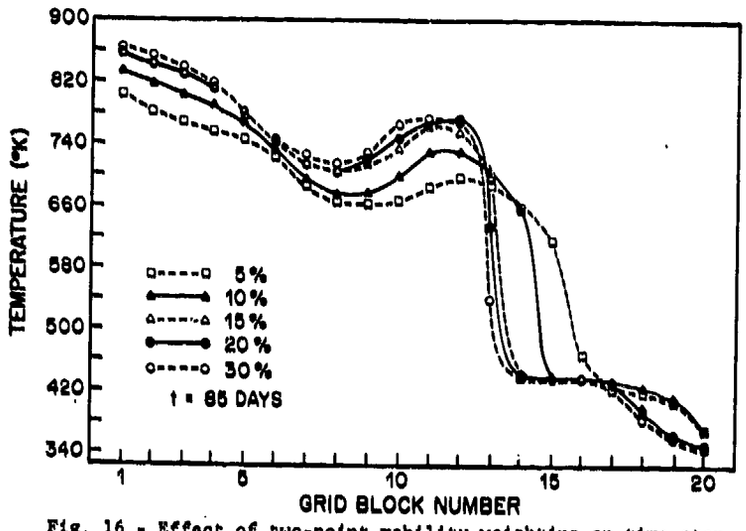

Fig. 16 - Effect of two-point mobility weighting on time step sensitivity. One-dimensional reservoir.

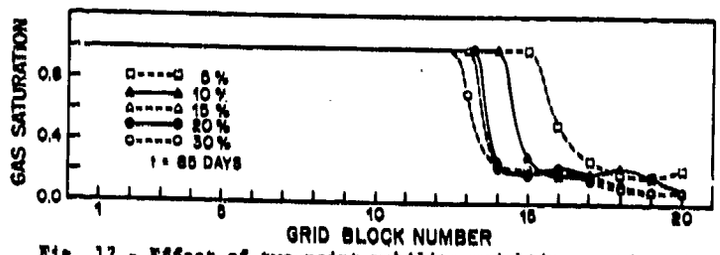

Fig. 17 - Effect of two-point mobility weighting on time step sensitivity. One-dimensional reservoir.

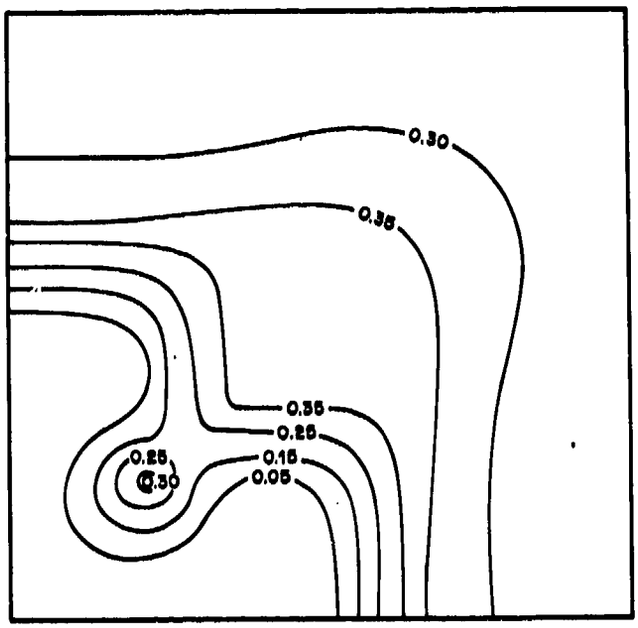

Fig. 18 - Water saturation profile. Time = 150 days. No harmonic weighting.

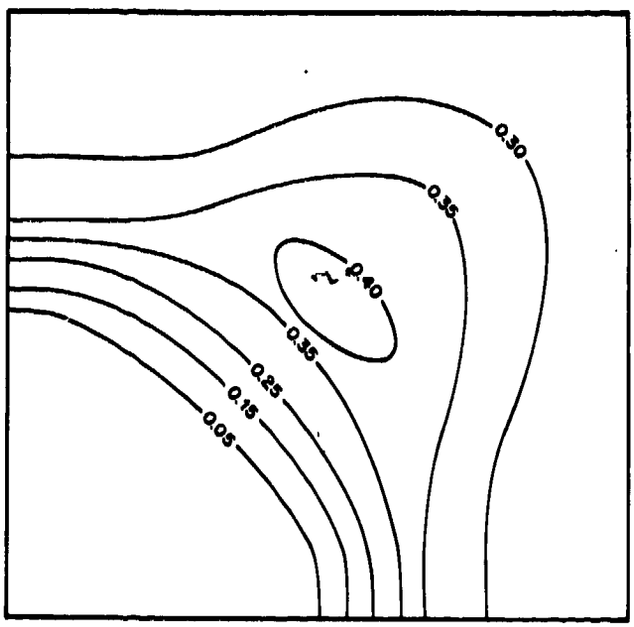

Fig. 19 - Water saturation profile. Time = 150 days. With harmonic weighting.

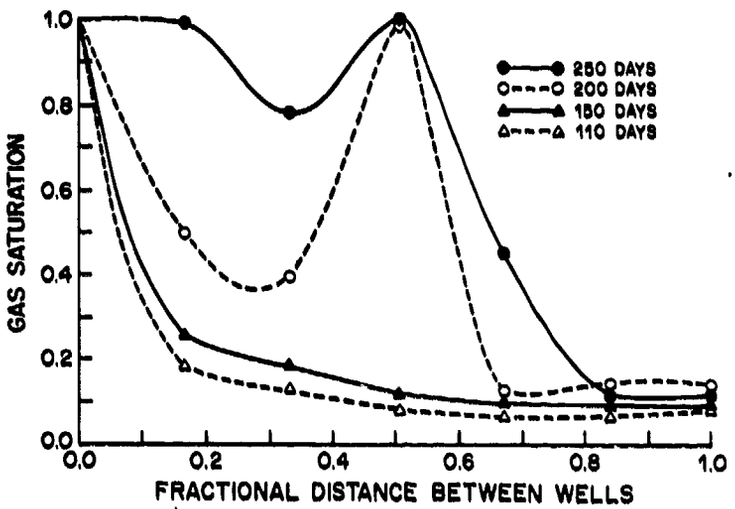

Fig. 20 - Diagonal cross-section of 1/4 five spot. No harmonic weighting.

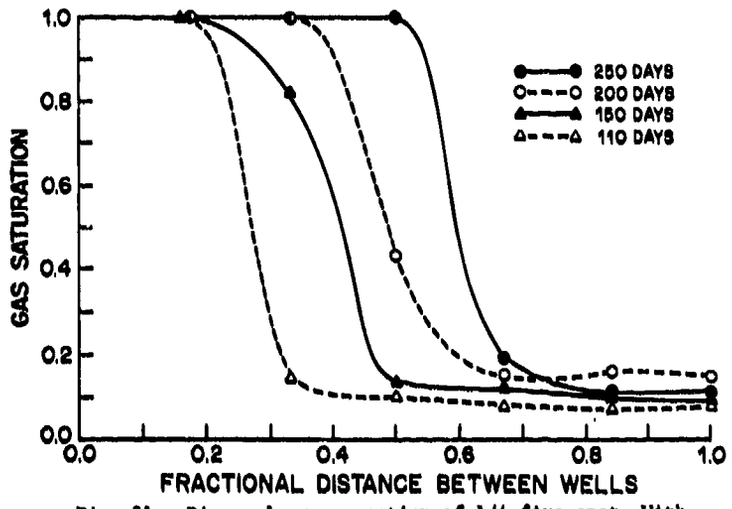

Fig. 21 - Diagonal cross-section of 1/4 five spot. With harmonic weighting.

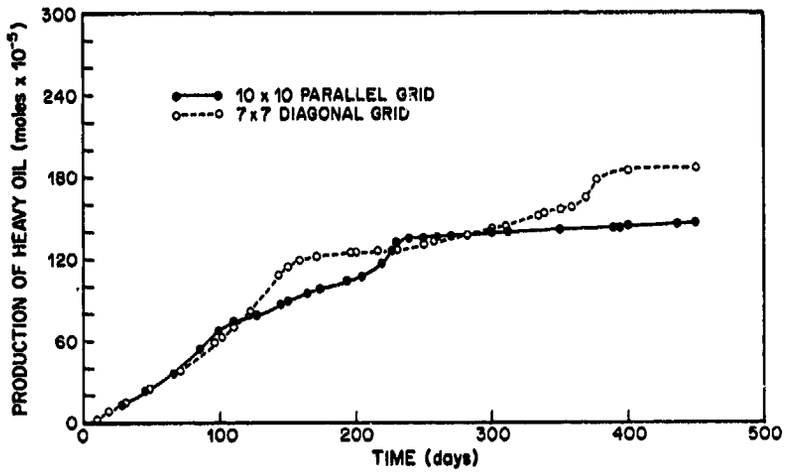

Fig. 22 - Comparison of parallel and diagonal grid direction. With harmonic weighting.

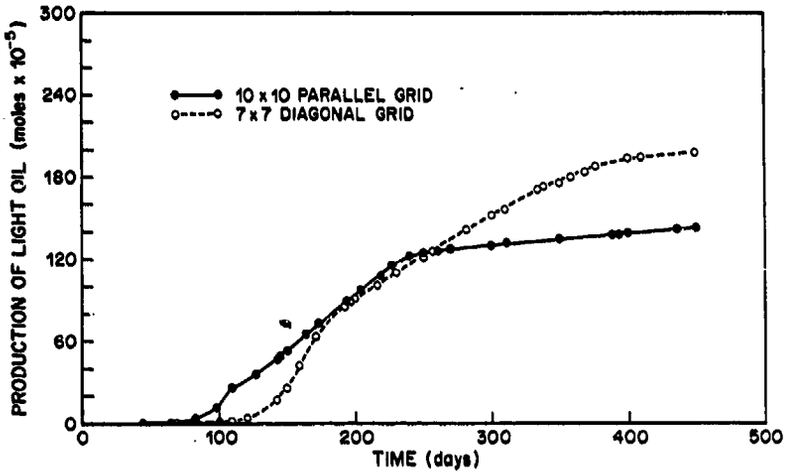

Fig. 23 - Comparison of parallel and diagonal grid direction. With harmonic weighting.